

Letter Report

Yucca Mountain Environmental Monitoring Systems Initiative
**Air Quality Scoping Study for Pahranagat National
Wildlife Refuge, Lincoln County, Nevada**



prepared by

Johann Engelbrecht, Ilias Kavouras, Dave Campbell,
Scott Campbell, Steven Kohl and David Shafer
Desert Research Institute
Nevada System of Higher Education

submitted to

Nevada Site Office
National Nuclear Security Administration
U.S. Department of Energy
Las Vegas, Nevada

July 2008

The work upon which this report is based was supported by the U.S. Department of Energy under Contract #DE-AC52-06NA26383.

Reference herein to any specific commercial product, process, or service by trade name, trademark, manufacturer, or otherwise, does not necessarily constitute or imply its endorsement, recommendation, or favoring by the United States Government or any agency thereof or its contractors or subcontractors. The views and opinions of authors expressed herein do not necessarily state or reflect those of the United States Government of any agency thereof.

This report has been reproduced directly from the best available copy.
Available for sale to the public, if paper, from:

U.S. Department of Commerce
National Technical Information Service
5285 Port Royal Road
Springfield, VA 22161
Phone: 800.553.6847
Fax: 703.605.6900
Email: orders@ntis.gov
Online ordering: <http://www.ntis.gov/ordering.htm>

Available electronically at <http://www.osti.gov/bridge>.

Available for a processing fee to the U.S. Department of Energy and its contractors, in paper, from:

U.S. Department of Energy
Office of Scientific and Technical Information
P.O. Box 62
Oak Ridge, TN 37831-0062
Phone: 865.576.8401
Fax: 865.576.5728
Email: reports@adonis.osti.gov

CONTENTS

| | |
|---|-----|
| LIST OF FIGURES | iii |
| LIST OF TABLES | iv |
| INTRODUCTION | 1 |
| SITE LOCATION AND CHARACTERISTICS | 1 |
| AEROSOL SAMPLING AND MONITORING | 2 |
| Filter Sampling | 2 |
| Sampler Description and Procedures | 2 |
| Gravimetry | 4 |
| Chemical Analysis | 6 |
| Aerosol Monitoring..... | 9 |
| Monitor Description and Procedures | 9 |
| Continuous Measurements of PM ₁₀ and PM _{2.5} | 11 |
| Comparison of Filter to Continuous Results..... | 16 |
| METEOROLOGY | 17 |
| Associations of Meteorology with Aerosol Measurements | 22 |
| CONCLUSIONS..... | 24 |
| ACKNOWLEDGEMENTS | 24 |
| REFERENCES | 24 |

LIST OF FIGURES

| | |
|--|----|
| 1. Southern Nevada map showing the location of Site #6 (at Pahranagat NWR), Nevada Test Site, and Yucca Mountain. | 1 |
| 2. Photographs of PQ100 (green/gray box in left photo), PQ200 (white box in left photo), and their sampling inlets (right photo)..... | 2 |
| 3. A diagrammatic representation of the BGI PM _{2.5} sampler showing the PM ₁₀ size selective impactor head as the first stage followed by a PM _{2.5} VSAC..... | 3 |
| 4. Time series of PM ₁₀ and PM _{2.5} mass concentrations (\pm uncertainty) at Site #6 (Pahranagat NWR)..... | 5 |
| 5. Relationship between mean (\pm uncertainty) daily PM _{2.5} and PM ₁₀ at Pahranagat NWR. | 5 |
| 6. Reconstructed mass for PM ₁₀ and PM _{2.5} based on chemical composition. | 9 |
| 7. Left photograph: The front panels of PM ₁₀ (right on the left photograph) and PM _{2.5} (left on the left photograph) of TEOM. Right photograph: The DUSTTRAK monitors (green) resting on top of the two TEOM measuring units..... | 10 |
| 8. Schematic drawing of the sampling inlet for the DUSTTRAK (not to scale). | 11 |
| 9. Mean 24-h PM ₁₀ and PM _{2.5} mass concentrations measured by TEOM at Site #6 (Pahranagat NWR)..... | 12 |
| 10. PM _{2.5} /PM ₁₀ mass ratios measured by TEOM at Site #6 (Pahranagat NWR). | 13 |
| 11. Variation of mean (\pm st.error) PM ₁₀ and PM _{2.5} ($\mu\text{g}/\text{m}^3$) in weekdays and weekends at Site #6 (Pahranagat NWR) (Monday=1, Tuesday=2, Wednesday=3, Thursday=4, Friday=5, Saturday=6, Sunday=7). | 13 |

| | |
|---|----|
| 12. PM ₁₀ mass ($\mu\text{g}/\text{m}^3$) measured with DUSTTRAK and TEOM at Site #6 (Pahranagat NWR)..... | 14 |
| 13. PM _{2.5} mass ($\mu\text{g}/\text{m}^3$) measured with DUSTTRAK and TEOM at Site #6 (Pahranagat NWR)..... | 15 |
| 14. Comparison of 24-h PM ₁₀ and PM _{2.5} mass concentrations measured by TEOM and DUSTTRAK. Error bars represent the standard error of the mean..... | 15 |
| 15. Relationships between PM ₁₀ concentrations ($\mu\text{g}/\text{m}^3$) measured by TEOM, DUSTTRAK, and filter-based methods..... | 16 |
| 16. Relationships between PM _{2.5} concentrations ($\mu\text{g}/\text{m}^3$) measured by TEOM, DUSTTRAK, and filter-based methods..... | 17 |
| 17. Solar radiation (in watts/ m^2) at Site #6 (Pahranagat NWR)..... | 18 |
| 18. Temperature (in °F) and relative humidity at Site #6 (Pahranagat NWR)..... | 18 |
| 19. Total precipitation (in mm) at Site #6 (Pahranagat NWR)..... | 19 |
| 20. Wind speed (in miles/hr) at Site #6 (Pahranagat NWR)..... | 19 |
| 21. Wind direction at Site #6 (Pahranagat NWR)..... | 20 |
| 22. Wind direction and speed at Pahranagat NWR..... | 21 |
| 23. Average wind speed for each wind direction sector..... | 21 |
| 24. Hourly variation of PM ₁₀ and PM _{2.5} mass concentrations ($\mu\text{g}/\text{m}^3$) as well as wind speed (miles/hour) at Site #6 (Pahranagat NWR)..... | 22 |
| 25. Mean (\pm st.error) of PM ₁₀ mass concentrations ($\mu\text{g}/\text{m}^3$) for different wind direction sectors at Site #6 (Pahranagat NWR)..... | 23 |
| 26. Mean (\pm st.error) of PM _{2.5} mass concentrations ($\mu\text{g}/\text{m}^3$) for different wind direction sectors at Site #6 (Pahranagat NWR)..... | 23 |

LIST OF TABLES

| | |
|---|----|
| 1. Longitude, latitude, and elevation of the mobile trailer location at Site #6 (Pahranagat NWR)..... | 2 |
| 2. Collection day, filter number, mass, and uncertainty determined by gravimetric analysis and associated flags of samples at Site #6 (Pahranagat NWR)..... | 4 |
| 3. Results of the chemical analysis for selected filters from Pahranagat NWR..... | 6 |
| 4. Statistics for 24-h PM ₁₀ and PM _{2.5} TEOM mass concentrations..... | 11 |
| 5. Descriptive statistics of 1-hour meteorological data..... | 17 |
| 6. Wind condition classifications..... | 20 |

INTRODUCTION

The Desert Research Institute (DRI) is performing a scoping study as part of the U.S. Department of Energy's Yucca Mountain Environmental Monitoring Systems Initiative (EMSI). The main objective is to obtain baseline air quality information for Yucca Mountain and an area surrounding the Nevada Test Site (NTS).

Air quality and meteorological monitoring and sampling equipment housed in a mobile trailer (shelter) is collecting data at eight sites outside the NTS, including Ash Meadows National Wildlife Refuge (NWR), Pahranagat NWR, Beatty, Rachel, Caliente, Crater Flat, and Tonopah Airport, and at four sites on the NTS (Engelbrecht *et al.*, 2007a-d). The trailer is stationed at any one site for approximately eight weeks at a time.

This letter report provides a summary of air quality and meteorological data on completion of the site's sampling program.

SITE LOCATION AND CHARACTERISTICS

The Pahranagat NWR is located east of Nellis Air Force Range and Desert NWR, along U.S. Route 93 in Lincoln County. It covers an area of 5,380 acres. The refuge has four main water bodies, North Marsh, Upper and Lower Pahranagat lakes, and Middle Marsh, that provide habitat to migratory birds flying along the Pacific Flyway. It is about 4 miles from the town of Alamo and 90 miles north of Las Vegas. The refuge is about 80 miles east of the Yucca Mountain repository (Figure 1).

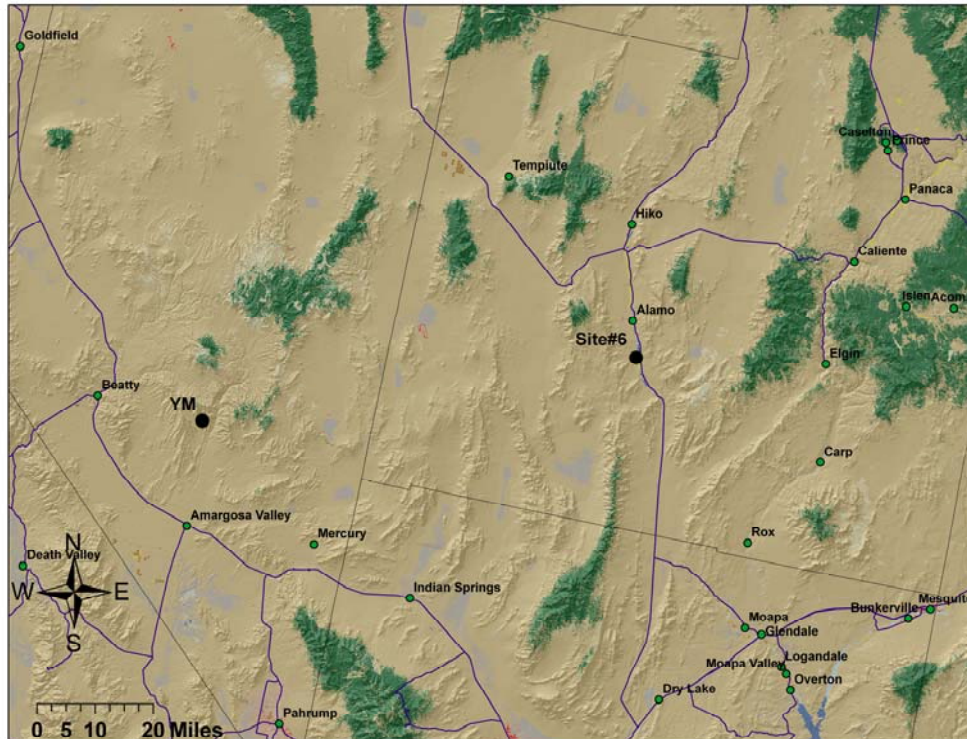


Figure 1. Southern Nevada map showing the location of Site #6 (at Pahranagat NWR), Nevada Test Site, and Yucca Mountain. The map background is land use and land cover from the 2001 National Land Cover Database.

The mobile trailer was located inside the Pahranagat NWR on the south end of the facilities area, about 1.5 miles west of the U.S. Route 93. Monitoring of PM₁₀, PM_{2.5}, and meteorological conditions was carried out from February 17, 2007, to April 18, 2007.

Table 1. Longitude, latitude, and elevation of the mobile trailer location at Site #6 (Pahranagat NWR).

| Site | Pahranagat NWR |
|-----------|----------------|
| Latitude | 37° 16' 5.53" |
| Longitude | 115° 7' 14.45" |

AEROSOL SAMPLING AND MONITORING

Filter Sampling

Sampler Description and Procedures

BGI, Inc., PQ100 and PQ200 Ambient PM_{2.5} Federal Reference Method (FRM) samplers were used to collect 24-h integrated PM₁₀ and PM_{2.5} samples. Figure 2 shows the PQ100 and PQ200 in the mobile trailer (left) and the PM₁₀ sampling inlets on the top of the trailer (right). Both the PQ100 (Designation No. RFPS-1298-124) and PQ200 (Designation No. RFPS-0498-116) samplers are designed to meet the criteria for collecting 24-h samples of ambient aerosol according to the U.S. National Ambient Air Quality Standards (NAAQS).

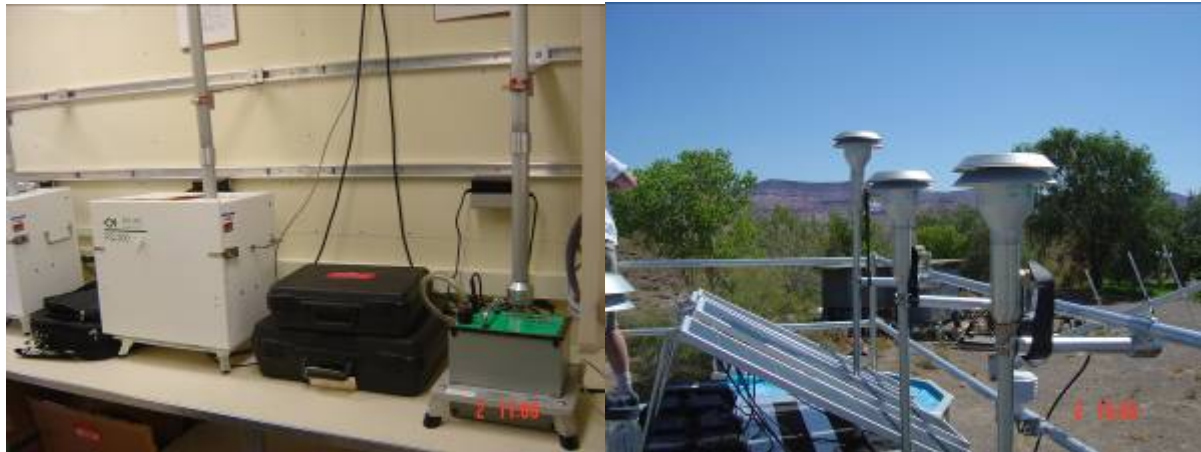


Figure 2. Photographs of PQ100 (green/gray box in left photo), PQ200 (white box in left photo), and their sampling inlets (right photo).

Figure 3 shows a schematic drawing of the samplers. Particles with aerodynamic diameter larger than 10 μm are removed by impaction by the size selective inlet, while the smaller particles remain airborne. The PM₁₀ fraction is collected by a filter located downstream of the size selective inlet. For the collection of PM_{2.5}, particles in the range between 2.5 and 10 μm were removed by the Very Sharp Cut Cyclone (VSCC) (U.S. Environmental Protection Agency [EPA] Equivalent Designation No. EQPM-0202-142), then collected on a filter.

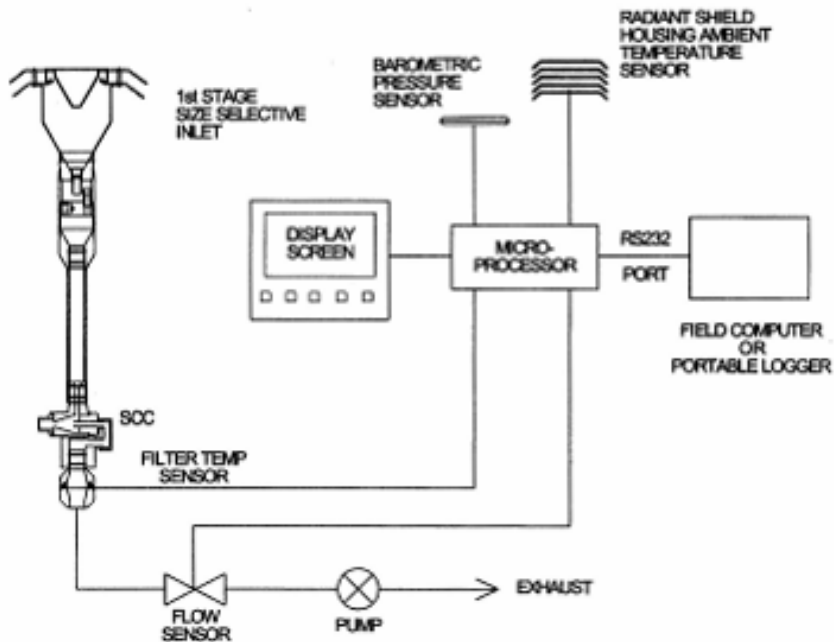


Figure 3. A diagrammatic representation of the BGI PM₁₀ sampler showing the PM₁₀ size selective impactor head as the first stage followed by a PM_{2.5} VSCC. This configuration can be readily modified to a PM₁₀ sampler by removal of the VSCC.

For both PQ100 and PQ200, samples were collected at a volumetric flow rate of 16.67 liters/min. The flow rate is controlled to ± 2 percent precision with a mass flow controller. The actual ambient temperature and barometric pressure, filter temperature and pressure, and anomalies (if any) were recorded by a microprocessor. The sampler was equipped to operate from an internal 12-volt DC battery. The battery was normally recharged from 120-volt AC. Alternatively, a 32-watt solar panel with an additional external ballast battery was installed to provide power for periods without electricity. Two sets of PQ100 and PQ200 samplers were installed in the mobile trailer. PM₁₀ and PM_{2.5} samples were collected on filters in numbered cassettes, labeled TT (for PM₁₀ Teflon), FT (for PM_{2.5} Teflon), TQ (for PM₁₀ Quartz), and FQ (for PM_{2.5} Quartz). Each filter cassette was loaded with a pre-weighed 46.2-mm-diameter PTFE (Teflon) membrane filter (Whatman # 7592-004) or 47-mm quartz fiber (Pallflex #2500QAT-UP) filter. The Teflon membrane collected particles for gravimetric analysis, light absorption by densitometry, and elements by X-ray fluorescence spectrometry. Quartz fiber filters were used for measurement of water-soluble ions by atomic absorption spectrometry, ion chromatography, and automated colorimetry, and also for measurement of carbon species by thermal optical reflectance.

Operation, calibration, and maintenance of PQ100 and PQ200 particulate samplers are described in standard operating procedure DRI SOP # 1-211.2 "BGI PQ100 PM10 and PQ200 PM2.5 REFERENCE SAMPLERS FOR THE YUCCA MOUNTAIN AIR QUALITY PROGRAM." Flow calibration and leak tests (only for PQ200) were performed on the day of installation (May 25, 2007). The leak check was performed according to the manufacturer's operational instruction manual only for PQ200; no manufacturer's procedure exists for the PQ100. The flow rates were set according to a BGI Tri-Cal NIST traceable

standard. The sampler was then placed in “calibration” or “run” mode and a one-point calibration verification or one-point flow-rate verification performed. Aerosol samples were collected on a 1-in-6-day schedule. Audits of the flow and leak tests were done onsite at the beginning and end of the monitoring campaign. Teflon and quartz filters were prepared and assembled in their filter holders by the Desert Research Institute’s (DRI) Environmental Analysis Facility (EAF) in Reno and shipped to DRI’s facilities in Las Vegas. The filters were kept at -4°C and transported to the field in a cryo-cooler. Exposed filters were also stored at -4°C in Las Vegas. Upon completion of the monitoring period at the site, all filters were shipped to the EAF in Reno.

Gravimetry

Table 2 shows mass concentrations (and uncertainty) of filters collected at Pahranagat NWR. PM₁₀ mass concentrations varied from 1.70 µg/m³ to 15.09 µg/m³, while PM_{2.5} mass concentrations ranged from 0.45 µg/m³ to 5.78 µg/m³. Similar temporal trends were observed for both PM₁₀ and PM_{2.5}. In all cases, 24-h PM₁₀ and PM_{2.5} levels were significantly lower than the daily and annual NAAQS as recently revised by EPA (24-h PM₁₀: 150 µg/m³, 24-h PM_{2.5}: 35 µg/m³; Annual PM_{2.5}: 15 µg/m³) (Figure 4). Fine particles (PM_{2.5}) accounted for approximately one-third of PM₁₀ (PM_{2.5}/PM₁₀ ratio of 0.37) (Figure 5).

Table 2. Collection day, filter number, mass, and uncertainty determined by gravimetric analysis and associated flags of samples at Site #6 (Pahranagat NWR).

| Date | No | Type | Mass (µg/m ³) | Uncertainty (µg/m ³) | Flags |
|-----------|-----|-------------------|------------------------------|-------------------------------------|--------------------------|
| 2/17/2007 | 071 | PM ₁₀ | 2.3691 | 0.4299 | |
| | | PM _{2.5} | 0.7907 | 0.4281 | |
| 2/23/2007 | 072 | PM ₁₀ | 1.7055 | 0.4290 | |
| | | PM _{2.5} | 0.4578 | 0.4279 | |
| 3/1/2007 | 074 | PM ₁₀ | 3.9101 | 0.4347 | |
| | | PM _{2.5} | 1.7478 | 0.4292 | |
| 3/7/2007 | 075 | PM ₁₀ | -99.9999 | -99.9999 | V: invalid (Void) sample |
| | | PM _{2.5} | 1.8310 | 0.4294 | |
| 3/13/2007 | 076 | PM ₁₀ | 7.2379 | 0.4514 | |
| | | PM _{2.5} | 1.3733 | 0.4287 | |
| 3/19/2007 | 077 | PM ₁₀ | 14.3511 | 0.5150 | |
| | | PM _{2.5} | 5.7844 | 0.4432 | |
| 3/25/2007 | 078 | PM ₁₀ | 7.3211 | 0.4520 | |
| | | PM _{2.5} | 3.7037 | 0.4342 | |
| 3/31/2007 | 079 | PM ₁₀ | 5.2413 | 0.4403 | |
| | | PM _{2.5} | 3.6636 | 0.4342 | |
| 4/6/2007 | 081 | PM ₁₀ | 6.4892 | 0.4469 | |
| | | PM _{2.5} | 4.0383 | 0.4355 | |
| 4/12/2007 | 082 | PM ₁₀ | 15.0998 | 0.5235 | |
| | | PM _{2.5} | 3.4555 | 0.4335 | |
| 4/18/2007 | 083 | PM ₁₀ | 4.1181 | 0.4355 | |
| | | PM _{2.5} | 3.2057 | 0.4327 | |

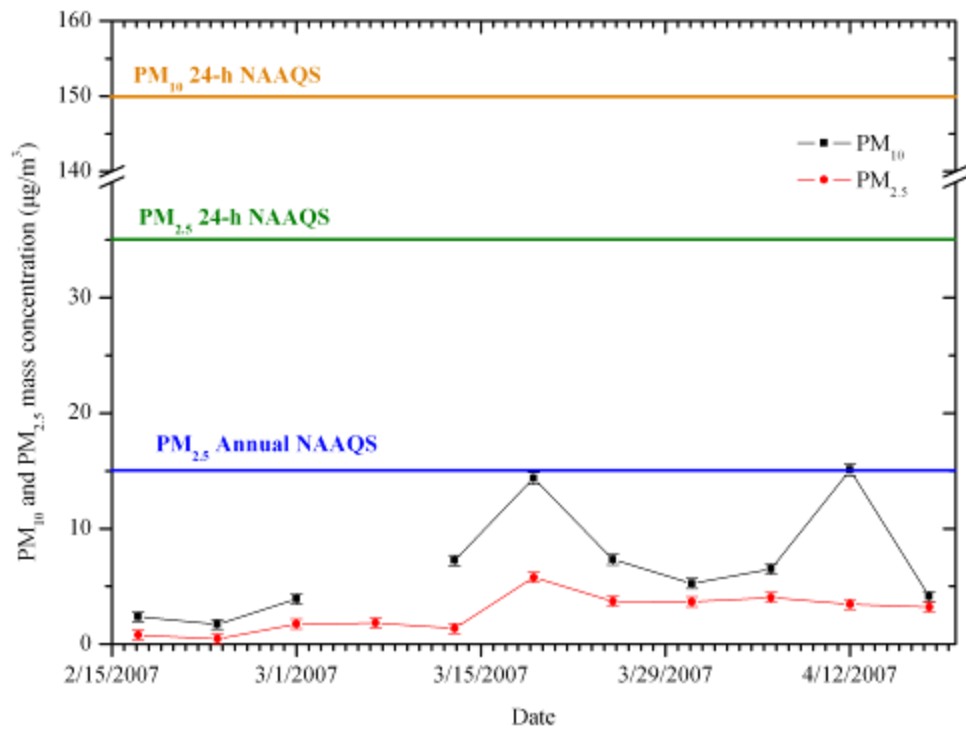


Figure 4. Time series of PM₁₀ and PM_{2.5} mass concentrations (\pm uncertainty) at Site #6 (Pahrangat NWR).

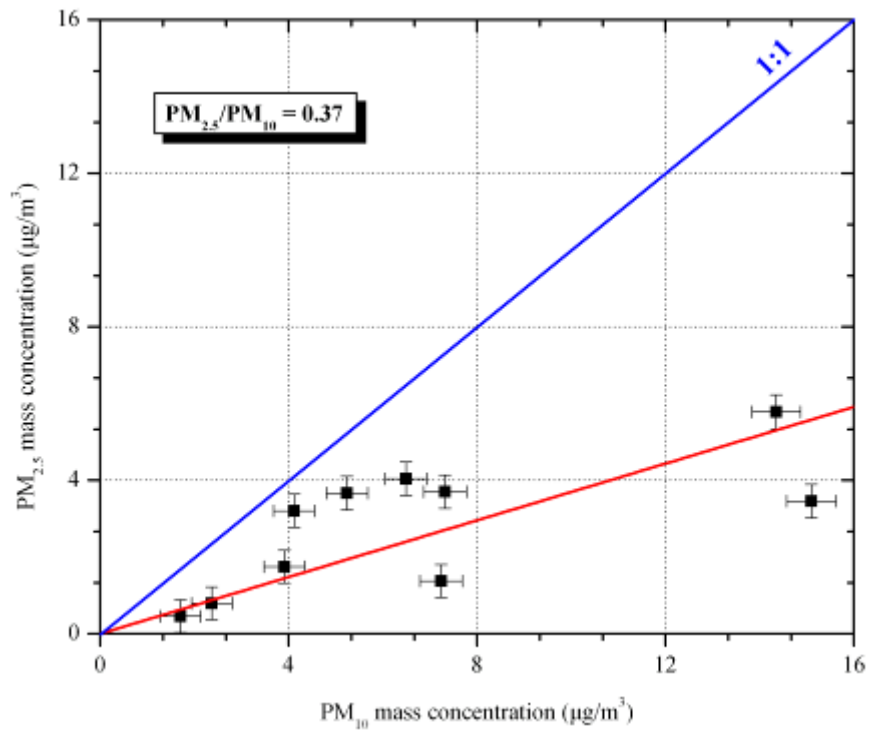


Figure 5. Relationship between mean (\pm uncertainty) daily PM_{2.5} and PM₁₀ at Pahrangat NWR.

Chemical Analysis

Table 3 shows the chemical content of PM₁₀ and PM_{2.5} samples collected on March 19, 2007 and April 6, 2007. Chemical analysis included elements (from sodium to uranium) with x-ray fluorescence spectrometry (XRF), major anions (sulfate, nitrate, and chloride) by ion chromatography (IC), major cations (sodium, potassium, calcium and magnesium) by atomic absorption (AA), particulate ammonium by automated colorimetry (AC), and elemental, organic and carbonate carbon by thermal optical reflectance (TOR).

Table 3. Results of the chemical analysis for selected filters from Pahrangat NWR. Chemical components with concentrations higher than two times the uncertainty are in bold, while those with concentrations lower than two times the uncertainty are in italics. Concentrations are in $\mu\text{g}/\text{m}^3$.

| SIZE | 3/19/2007 | | | | 4/06/2007 | | | |
|---|------------------|---------------|-------------------|---------------|------------------|---------------|-------------------|---------------|
| | PM ₁₀ | | PM _{2.5} | | PM ₁₀ | | PM _{2.5} | |
| | Conc. | Uncer. | Conc. | Uncer. | Conc. | Uncer. | Conc. | Uncer. |
| Mass | 14.3511 | 0.5150 | 5.7844 | 0.4432 | 6.4892 | 0.4469 | 4.0383 | 0.4355 |
| Chloride, Cl ⁻ | 0.0500 | 0.0297 | 0 | 0.0294 | 0.0313 | 0.0295 | 0 | 0.0294 |
| Nitrate, NO ₃ ⁻ | 0.4887 | 0.0335 | 0.1380 | 0.0299 | 0.2508 | 0.0306 | 0.0660 | 0.0296 |
| Sulfate, SO ₄ ²⁻ | 1.2438 | 0.0400 | 1.0185 | 0.0368 | 0.7491 | 0.0336 | 0.6301 | 0.0325 |
| Ammonium, NH ₄ ⁺ | 0.4569 | 0.0338 | 0.4119 | 0.0331 | 0.2433 | 0.0308 | 0.2368 | 0.0308 |
| Sodium, Na ⁺ | 0.1391 | 0.0066 | 0.0431 | 0.0057 | 0.0623 | 0.0058 | 0.0252 | 0.0056 |
| Magnesium, Mg ²⁺ | 0.065 | 0.0021 | 0.0135 | 0.0012 | 0.0392 | 0.0016 | 0.0111 | 0.0012 |
| Potassium, K ⁺ | 0.0737 | 0.0035 | 0.0326 | 0.0031 | 0.0437 | 0.0031 | 0.0186 | 0.003 |
| Calcium, Ca ₂₊ | 0.8536 | 0.0258 | 0.1039 | 0.0155 | 0.4952 | 0.0195 | 0.0866 | 0.0154 |
| OC1 | 0.2095 | 0.0838 | 1.0311 | 0.4003 | 0.2881 | 0.1136 | 0.6311 | 0.2456 |
| OC2 | 0.5776 | 0.1475 | 0.7292 | 0.1788 | 0.6017 | 0.1524 | 0.5754 | 0.147 |
| OC3 | 0.6336 | 0.1825 | 0.4955 | 0.1721 | 0.4965 | 0.1721 | 0.2038 | 0.1542 |
| OC4 | 0.3789 | 0.0659 | 0.2427 | 0.0582 | 0.2437 | 0.0582 | 0.1089 | 0.0531 |
| Pyrolyzed OC-TT | 0.3197 | 0.1149 | 0.0956 | 0.0492 | 0.1755 | 0.0703 | 0.0440 | 0.0399 |
| Pyrolyzed OC-Op | 0.2266 | 0.0885 | 0.0447 | 0.0402 | 0.1697 | 0.0707 | 0.0365 | 0.0392 |
| Total OC | 2.0261 | 0.2851 | 2.5432 | 0.3178 | 1.7995 | 0.2717 | 1.5556 | 0.2583 |
| EC1 | 0.3520 | 0.0848 | 0.1865 | 0.0507 | 0.3460 | 0.0835 | 0.0982 | 0.0356 |
| EC2 | 0.0763 | 0.0438 | 0.0645 | 0.0414 | 0.0232 | 0.0356 | 0 | 0.0347 |
| EC3 | 0 | 0.0115 | 0 | 0.0115 | 0 | 0.0115 | 0 | 0.0115 |
| Total EC | 0.2017 | 0.0585 | 0.2063 | 0.0591 | 0.1995 | 0.0582 | 0.0617 | 0.0455 |
| Total Carbon | 2.4285 | 0.3281 | 2.7705 | 0.3510 | 2.1234 | 0.3087 | 1.6173 | 0.2793 |
| Carbonate Carbon (CO ₃ ²⁻) | 0.2007 | 0.2225 | 0.0211 | 0.2150 | 0.1244 | 0.2178 | 0 | 0.215 |
| Sodium, Na | 0.1219 | 0.0822 | 0.0815 | 0.0816 | 0.0617 | 0.0812 | 0.0376 | 0.0810 |
| Magnesium, Mg | 0.1460 | 0.0438 | 0.0603 | 0.0433 | 0.0540 | 0.0432 | 0.0695 | 0.0433 |
| Aluminum, Al | 0.4268 | 0.0124 | 0.1276 | 0.0081 | 0.1902 | 0.0087 | 0.1475 | 0.0083 |
| Silicon, Si | 1.1361 | 0.0264 | 0.3287 | 0.0113 | 0.5170 | 0.0145 | 0.3567 | 0.0118 |
| Phosphorous, P | 0.0184 | 0.0030 | 0.0135 | 0.0030 | 0.0088 | 0.003 | 0.0075 | 0.003 |
| Sulfur, S | 0.3780 | 0.0151 | 0.3434 | 0.0146 | 0.2261 | 0.0134 | 0.2059 | 0.0132 |
| Chlorine, Cl | 0.0057 | 0.0016 | 0 | 0.0016 | 0.0016 | 0.0016 | 0 | 0.0016 |
| Potassium, K | 0.2440 | 0.0052 | 0.0823 | 0.0023 | 0.1092 | 0.0027 | 0.0753 | 0.0022 |
| Calcium, Ca | 0.7444 | 0.0152 | 0.1783 | 0.0041 | 0.3030 | 0.0065 | 0.1851 | 0.0042 |
| Scandium, Sc | 0 | 0.0058 | 0.0020 | 0.0058 | 0 | 0.0058 | 0 | 0.0058 |
| Titanium, Ti | 0.0375 | 0.0014 | 0.0086 | 0.0011 | 0.0143 | 0.0011 | 0.0096 | 0.0011 |

Table 4. Results of the chemical analysis for selected filters from Pahrangat NWR. Chemical components with concentrations higher than two times the uncertainty are in bold, while those with concentrations lower than two times the uncertainty are in italics. Concentrations are in $\mu\text{g}/\text{m}^3$ (continued).

| SIZE | 3/19/2007 | | | | 4/06/2007 | | | |
|----------------|------------------|---------------|-------------------|---------------|------------------|---------------|-------------------|---------------|
| | PM ₁₀ | | PM _{2.5} | | PM ₁₀ | | PM _{2.5} | |
| | Conc. | Uncer. | Conc. | Uncer. | Conc. | Uncer. | Conc. | Uncer. |
| Vanadium, V | 0.0006 | 0.0001 | 0.0002 | 0.0001 | 0.0004 | 0.0001 | 0.0001 | 0.0001 |
| Chromium, Cr | 0 | 0.001 | 0 | 0.001 | 0 | 0.001 | 0 | 0.001 |
| Manganese, Mn | 0.0088 | 0.0022 | 0 | 0.0021 | 0.0021 | 0.0021 | 0 | 0.0021 |
| Iron, Fe | 0.3476 | 0.0077 | 0.0733 | 0.0034 | 0.1148 | 0.0039 | 0.0768 | 0.0034 |
| Cobalt, Co | 0 | 0.0001 | 0 | 0.0001 | 0 | 0.0001 | 0 | 0.0001 |
| Nickel, Ni | 0 | 0.0006 | 0 | 0.0006 | 0 | 0.0006 | 0 | 0.0006 |
| Copper, Cu | 0.0012 | 0.0009 | 0.0009 | 0.0009 | 0.0003 | 0.0009 | 0.0086 | 0.0009 |
| Zinc, Zn | 0.0049 | 0.0009 | 0.0030 | 0.0009 | 0.0017 | 0.0009 | 0.0058 | 0.0009 |
| Gallium, Ga | 0 | 0.0031 | 0 | 0.0031 | 0 | 0.0031 | 0 | 0.0031 |
| Arsenic, As | 0 | 0.0001 | 0 | 0.0001 | 0 | 0.0001 | 0 | 0.0001 |
| Selenium, Se | 0.0035 | 0.0021 | 0 | 0.0021 | 0 | 0.0021 | 0 | 0.0021 |
| Bromine, Br | 0.0033 | 0.0015 | 0.0032 | 0.0015 | 0.0019 | 0.0015 | 0.0017 | 0.0015 |
| Rubidium, Rh | 0.0016 | 0.0011 | 0 | 0.0011 | 0 | 0.0011 | 0 | 0.0011 |
| Strontium, Sr | 0.0058 | 0.0020 | 0.0021 | 0.0020 | 0.0022 | 0.0020 | 0.0003 | 0.0020 |
| Yttrium, Y | 0.0008 | 0.0015 | 0.0006 | 0.0015 | 0.0001 | 0.0015 | 0.001 | 0.0015 |
| Zirconium, Zr | 0 | 0.0034 | 0.0015 | 0.0034 | 0 | 0.0034 | 0 | 0.0034 |
| Niobium, Nb | 0 | 0.0026 | 0.0018 | 0.0026 | 0 | 0.0026 | 0 | 0.0026 |
| Molybdenum, Mo | 0 | 0.0024 | 0 | 0.0024 | 0.0004 | 0.0024 | 0.0005 | 0.0024 |
| Palladium, Pd | 0 | 0.0045 | 0 | 0.0045 | 0.0030 | 0.0045 | 0.0008 | 0.0045 |
| Silver, Ag | 0.0002 | 0.0041 | 0 | 0.0041 | 0.0009 | 0.0041 | 0.0027 | 0.0041 |
| Cadmium, Cd | 0 | 0.0052 | 0.0010 | 0.0052 | 0 | 0.0052 | 0 | 0.0052 |
| Indium, In | 0 | 0.003 | 0.0001 | 0.003 | 0 | 0.003 | 0 | 0.003 |
| Tin, Sn | 0 | 0.0039 | 0 | 0.0039 | 0 | 0.0039 | 0.0022 | 0.0039 |
| Antimony, Sb | 0 | 0.0073 | 0.0046 | 0.0073 | 0.0001 | 0.0073 | 0.0003 | 0.0073 |
| Cesium, Cs | 0 | 0.0012 | 0 | 0.0012 | 0 | 0.0012 | 0 | 0.0012 |
| Barium, Ba | 0 | 0.0006 | 0 | 0.0006 | 0.0002 | 0.0006 | 0 | 0.0006 |
| Lanthanum, La | 0 | 0.0009 | 0 | 0.0009 | 0 | 0.0009 | 0 | 0.0009 |
| Cerium, Ce | 0 | 0.0013 | 0 | 0.0013 | 0 | 0.0013 | 0 | 0.0013 |
| Samarium, Sa | 0 | 0.0018 | 0.0006 | 0.0018 | 0 | 0.0018 | 0 | 0.0018 |
| Europium, Eu | 0.0006 | 0.0064 | 0.0004 | 0.0064 | 0 | 0.0064 | 0.0038 | 0.0064 |
| Terbium, Tb | 0 | 0.0024 | 0 | 0.0024 | 0 | 0.0024 | 0 | 0.0024 |
| Hafnium, Hf | 0 | 0.0139 | 0.0041 | 0.014 | 0 | 0.0139 | 0 | 0.0139 |
| Tantalum, Ta | 0 | 0.0117 | 0 | 0.0117 | 0.0018 | 0.0117 | 0.0045 | 0.0117 |
| Tungsten, W | 0 | 0.0168 | 0 | 0.0168 | 0 | 0.0168 | 0.0091 | 0.0168 |
| Iridium, Ir | 0 | 0.0036 | 0 | 0.0036 | 0 | 0.0036 | 0 | 0.0036 |
| Gold, Au | 0 | 0.0078 | 0.0016 | 0.0078 | 0 | 0.0078 | 0 | 0.0078 |
| Mercury, Hg | 0 | 0.0024 | 0 | 0.0024 | 0 | 0.0024 | 0 | 0.0024 |
| Thallium, Th | 0 | 0.0025 | 0 | 0.0025 | 0 | 0.0025 | 0 | 0.0025 |
| Lead, Pb | 0 | 0.0025 | 0.0023 | 0.0026 | 0 | 0.0025 | 0 | 0.0025 |
| Uranium, U | 0 | 0.0041 | 0.0010 | 0.0041 | 0 | 0.0041 | 0.0017 | 0.0041 |

OC = organic carbon

EC = elemental carbon

OP = optical pyrolysis

TT = transmittance

With respect to the chemical composition of PM₁₀ and PM_{2.5}, the following patterns are observed:

- Sulfur (S) was mostly in the form of sulfate (SO₄²⁻) with a sulfate-to-sulfur ratio of 2.97 to 3.31. Sulfate and ammonium were almost entirely (81 to 84 percent for sulfate, 100 percent for ammonium) associated with fine particles, while less than 30 percent of nitrate (26 to 28 percent) was measured in PM_{2.5}. Ammonium-to-sulfate molar ratios varied from 1.73 to 2.16, suggesting that sulfate aerosols were mostly in the form of ammonium bisulfate, (NH₄)HSO₄ (Malm *et al.*, 2002). Only a minor fraction (if any) of nitrates appeared to be neutralized by ammonium in the fine particle mode.
- Carbonaceous aerosol was predominantly in fine particles. For PM_{2.5}, organic carbon (OC) concentrations accounted for 54 to 69 percent of particle mass. The EC/OC ratio was lower than 0.10, which was suggestive of biogenic organic aerosol, either primary, through erosion of the epicuticular waxes of the leaves, or secondary, through the oxidation of naturally emitted terpenes (Kavouras *et al.*, 1998, 2000).
- Soluble potassium (K⁺) accounted for 30 to 40 percent of total potassium in PM₁₀ and for 25 to 40 percent of total potassium in PM_{2.5}. Soluble potassium is a tracer of biomass burning and/or salts from desert soils. This was further supported by the estimates of nonsoil potassium K_{non-soil} (K_{total}-(0.26 x [Al])) that were comparable to measured water-soluble K⁺.
- Ratios of Al/Si (0.37 to 0.41), K/Fe (0.70 to 1.12), and Al/Ca (0.50 to 0.80) were comparable to those determined for samples collected at the Interagency Monitoring of Protected Visibility Environments (IMPROVE) sites in the western United States (Al/Si: 0.31 to 0.43, K/Fe: 0.67 to 0.78, Al/Ca: 1.4 to 1.7) when soil dust was the major component of particulate matter (Kavouras *et al.*, 2005).

The IMPROVE mass estimation scheme is adopted to reconstruct aerosol mass into five major types: sulfate, nitrate, organic, light-absorbing carbon, and soil. For this scheme, sulfate and nitrate are assumed to be in the forms of ammonium sulfate [(NH₄)₂SO₄] and ammonium nitrate [NH₄NO₃], respectively (Malm *et al.*, 2004). Organic mass concentration [OMC] was estimated as [OMC] = 1.4 x [OC], where [OC] is the organic carbon concentration. The 1.4 factor was used to correct for other elements (mainly hydrogen and oxygen) associated with the composition of organic compounds (White and Roberts, 1977). Soil mass concentration [SOIL] was estimated as the sum of the elements present in the soil as oxides (Al₂O₃, SiO₂, CaO, K₂O, FeO, Fe₂O₃, and TiO₂) as follows:

[SOIL] = 2.2 x [Al] + 2.49 [Si] + 1.63 x [Ca] + 2.42 x [Fe] + 1.94 x [Ti]. Therefore, the reconstructed aerosol mass was estimated as follows:

$$[\text{Aerosol Mass}] = (128/96) x [\text{SO}_4] + (80/62) x [\text{NO}_3] + \text{EC} + [\text{OMC}] + [\text{SOIL}]$$

Figure 6 shows the concentrations of ammonium sulfate, ammonium nitrate, organic carbon mass, elemental carbon and soil for PM₁₀ and PM_{2.5} collected on 3/19/2007 and 4/06/2007 in Pahranagat NWR. Considering the positive bias for organic carbon measurements:

- Reconstructed particle mass accounted for 78 to 101 percent of measured PM₁₀ mass and for 119 to 121 percent of PM_{2.5} mass.
- Carbonaceous aerosol (OMC and EC) appeared to account for 21 to 43 percent of PM₁₀ and 56 to 66 percent of PM_{2.5}.
- Soil represented 39 to 41 percent of PM₁₀ and for 29 to 43 percent of PM_{2.5} mass, while sulfate contributed between 12 and 15 percent on PM₁₀ and 21 to 23 percent on PM_{2.5} (Figure 6).
- The differences of PM₁₀ and PM_{2.5} fractions are due to higher concentration of soil elements in the coarse fraction (particles with diameter between 2.5 and 10 μm).

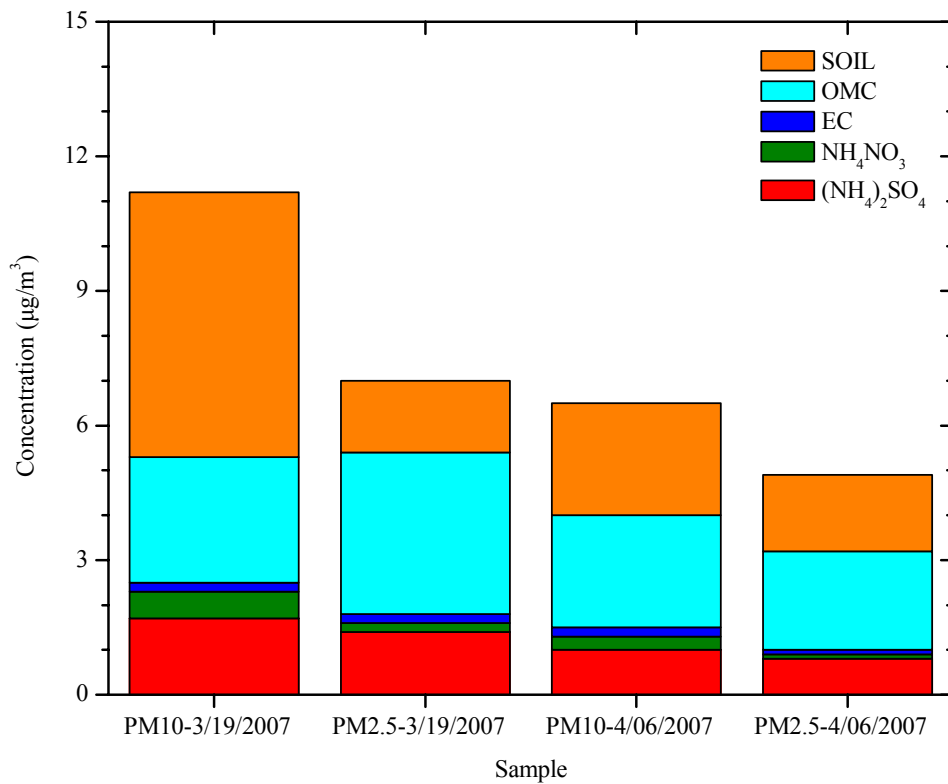


Figure 6. Reconstructed mass for PM₁₀ and PM_{2.5} based on chemical composition.

Aerosol Monitoring

Monitor Description and Procedures

The TEOM Series 1400 Ambient Particulate Monitor from Thermo Scientific and the DUSTTRAK™ Aerosol Monitor from TSI were used to continuously measure PM₁₀ and PM_{2.5} mass concentrations (Figure 7). The TEOM Series 1400 monitors the ambient particulate mass concentration of PM₁₀ (EPA certification EQPM-1090-079) or PM_{2.5} in real time by direct measurement of particulate mass collected on a filter attached to an oscillating inertial mass transducer. The mass transducer in the sensor unit has a tapered ceramic tube (element) that is fixed at the downstream end and a Teflon-coated glass fiber filter on the free end. The oscillating frequency of the tube changes proportionally as ambient air is drawn

through the filter and the particulate loading thereon increases. The flow-rate through the filter sample is set at a nominal 3.0 liters/min. A bypass (auxiliary) flow provides an additional 13.67 liters/min for a total flow-rate of 16.67 liters/min. An internal datalogger stores mass values, time, and some meteorological data. To eliminate bias caused by humidity, the filter is heated to 50°C. Operation, calibration, and maintenance of the TEOM are described in SOP 4.111-2 “RUPPRECHT & PATASHNICK (R&P), SERIES 1400A TAPERED ELEMENT OSCILLATING MICROBALANCE (TEOM).” Flow calibration and leak tests were performed on the day of installation (February 17, 2007). Data were downloaded during site visits. Regular checks of time, filter loading, by-pass filter, and flow rates were accomplished during site visits.



Figure 7. Left photograph: The front panels of PM₁₀ (right on the left photograph) and PM_{2.5} (left on the left photograph) of TEOM. Right photograph: The DUSTTRAK monitors (green) resting on top of the two TEOM measuring units

The DUSTTRAK™ Aerosol Monitor is a portable, battery operated laser photometer. The monitor provides measurements of particle mass based on light scattering. Atmospheric aerosol passes through a size selective inlet (either PM₁₀ or PM_{2.5}) and is directed to an optics chamber at a flow rate of 1.7 liters/min. The light source is a laser diode that emits light at a wavelength of 780 nm. The aerosol sample is drawn into the sensing chamber where it is illuminated with a narrow beam of laser light. Light scattered by aerosol particles is collected by a set of lenses and focused onto the photodetector. The detector signal is proportional to the amount of scattered light, which is proportional to the mass concentration of the aerosol. Voltage is read by the processor and multiplied by an internal calibration constant to yield mass concentration. The calibration constant is pre-set by the manufacturer for scattering characteristics of the respirable mass of ISO 12103-1 Al test dust. Local variations in aerosol particle size distribution and composition relative to this standard may result in differences in the actual response factor of the instrument. The operation, calibration, and maintenance of the DUSTTRAK are described in SOP DRI 1.211-2 “TSI INCORPORATED MODEL 8520 DUSTTRAK AEROSOL MONITOR FOR THE YUCCA MOUNTAIN AIR QUALITY PROGRAM.”

Both PM₁₀ and PM_{2.5} DUSTTRAK inlets were attached on a wide “Y” connector, which was connected to one end of a second “Y” (Figure 8). A funnel was connected to the

other end of the second “Y” to achieve fast exchange of ambient air into the sampling line. Flow calibration and zero-test were performed on the day of installation (February 17, 2007) and subsequent site visits. Deviations in flow were predominantly due to failure of the pump diaphragm. In those cases, the instrument was replaced. Deviations of the zero check were corrected by performing zero calibration according to the manufacturer’s operational instruction manual.

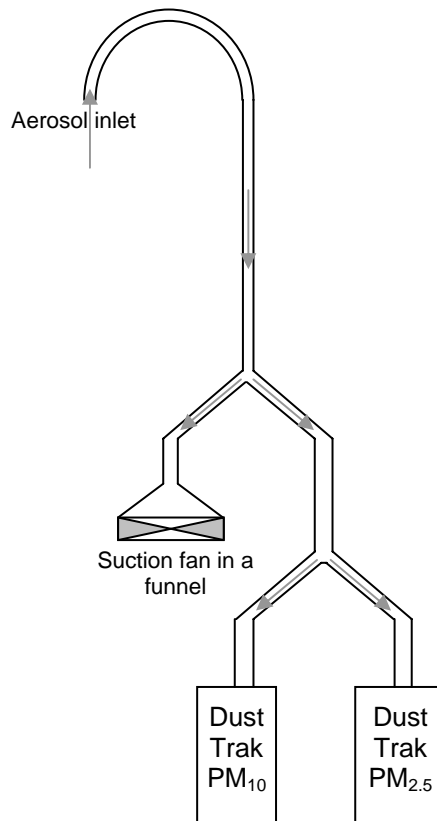


Figure 8. Schematic drawing of the sampling inlet for the DUSTTRAK (not to scale).

Continuous Measurements of PM₁₀ and PM_{2.5}

Trends and correlations of particle mass are examined using hourly TEOM data integrated for 24 hours (from 0:00. to 23:59). Statistics of 24-h particle mass are presented in Table 4.

Table 4. Statistics for 24-h PM₁₀ and PM_{2.5} TEOM mass concentrations.

| | Mean | Median | Minimum | Maximum | Std. Deviation |
|-------------------|------|--------|---------|---------|----------------|
| PM ₁₀ | 12.2 | 11.2 | 3.5 | 34.5 | 5.9 |
| PM _{2.5} | 2.3 | 2.1 | 0.0 | 7.4 | 1.6 |

Twenty-four-h PM₁₀ levels ranged from 3.5 to 34.5 $\mu\text{g}/\text{m}^3$, with a mean of 12.2 ($\sigma=5.9$) $\mu\text{g}/\text{m}^3$, while PM_{2.5} concentrations varied from 0.0 to 7.4 $\mu\text{g}/\text{m}^3$, with a mean of 2.3 ($\sigma=1.6$) $\mu\text{g}/\text{m}^3$ (Figure 9). Similar temporal trends were found for PM₁₀ and PM_{2.5} at Pahrangat NWR. A consistent relationship between PM fractions was observed during the monitoring period, with fine particles accounting for about one-fourth of PM₁₀ (PM_{2.5}/PM₁₀ ratio of 0.17) (Figure 10). While differences in particle mass for weekdays/weekends were not statistically significant, somewhat higher PM₁₀ levels were measured for Saturdays (Day #6) (Figure 11).

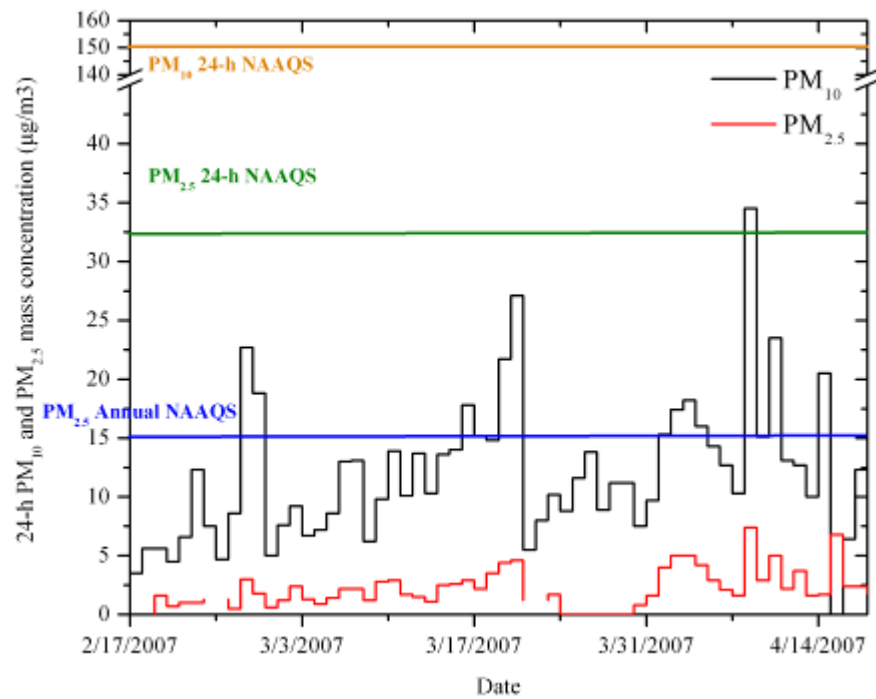


Figure 9. Mean 24-h PM₁₀ and PM_{2.5} mass concentrations measured by TEOM at Site #6 (Pahrangat NWR).

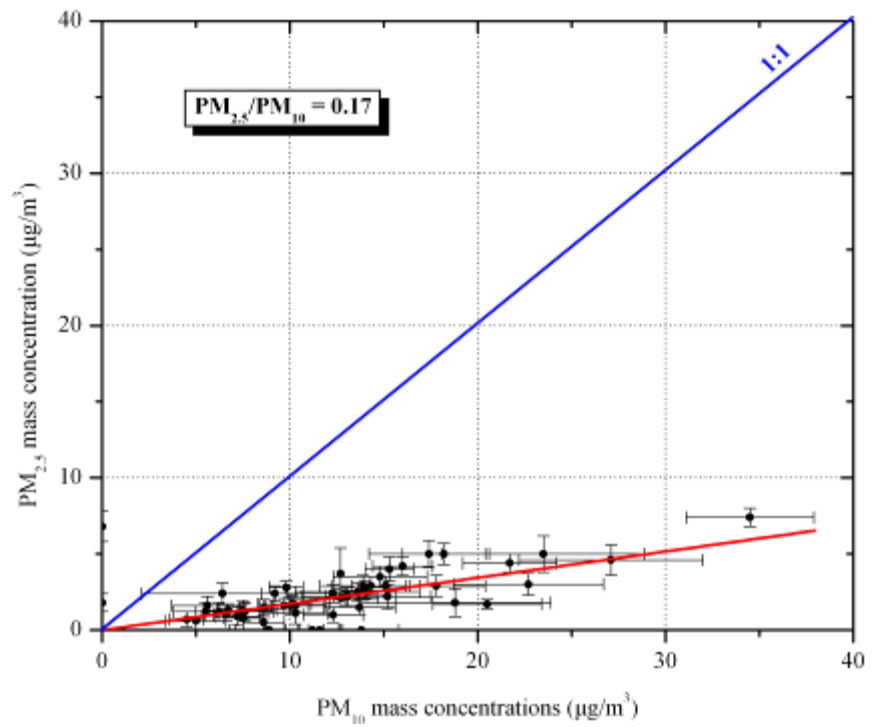


Figure 10. $\text{PM}_{2.5}/\text{PM}_{10}$ mass ratios measured by TEOM at Site #6 (Pahrangat NWR). Error bars represent the standard error of the mean.

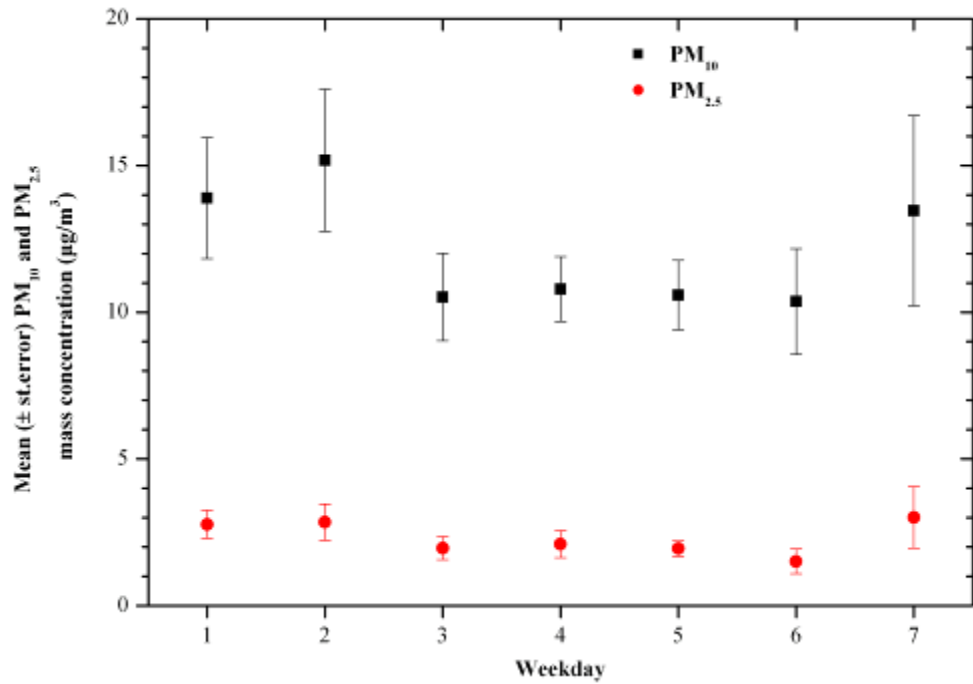


Figure 11. Variation of mean (\pm st.error) PM_{10} and $\text{PM}_{2.5}$ ($\mu\text{g}/\text{m}^3$) in weekdays and weekends at Site #6 (Pahrangat NWR) (Monday=1, Tuesday=2, Wednesday=3, Thursday=4, Friday=5, Saturday=6, Sunday=7).

Variations of daily PM_{10} and $PM_{2.5}$ measured with DUSTTRAK and TEOM are presented in Figure 12 and Figure 13. The absolute differences between concentrations measured by DUSTTRAK and TEOM were larger for PM_{10} as compared to those for $PM_{2.5}$. Daily trends of particle mass concentrations measured by DUSTTRAK and TEOM were comparable for PM_{10} mass. DUSTTRAK S/N 85200784 was running until March 18, 2007, and DUSTTRAK S/N 85200794 was operating for the remaining period for PM_{10} monitoring. The time series plots for PM_{10} particle mass concentrations measured by TEOM and DUSTTRAK are somewhat comparable in shape. The temporal correlations between DUSTTRAK and TEOM were low ($R=-0.02$ to 0.35). A slope of 1.77964 and an intercept of $7.50064 \mu\text{g}/\text{m}^3$ (Figure 14) were computed for PM_{10} . This was indicative of the weakness of the light-scattering technique to monitor dust particles. As for $PM_{2.5}$, the slope between TEOM and DUSTTRAK $PM_{2.5}$ was -0.0134 with a rather low intercept of $1.64142 \mu\text{g}/\text{m}^3$.

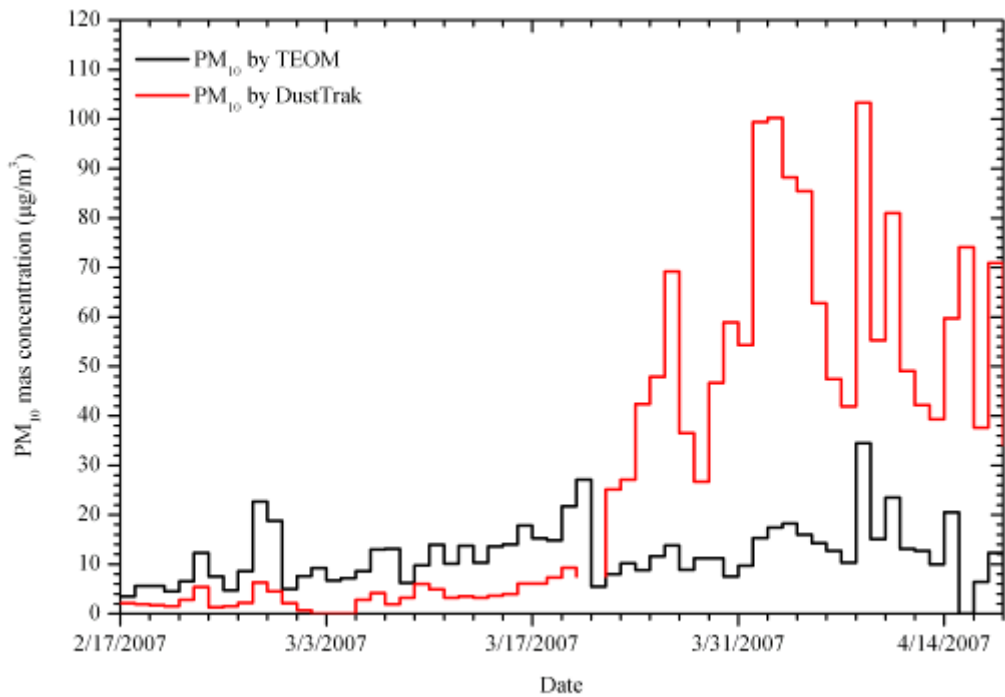


Figure 12. PM_{10} mass ($\mu\text{g}/\text{m}^3$) measured with DUSTTRAK and TEOM at Site #6 (Pahranagat NWR).

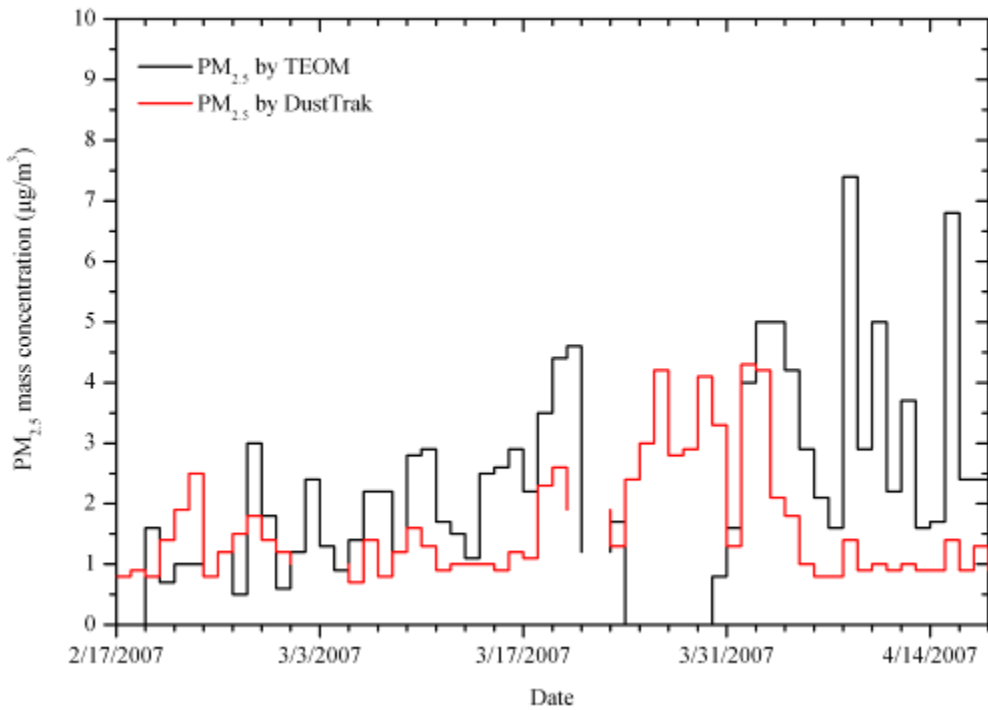


Figure 13. PM_{2.5} mass ($\mu\text{g}/\text{m}^3$) measured with DUSTTRAK and TEOM at Site #6 (Pahranagat NWR).

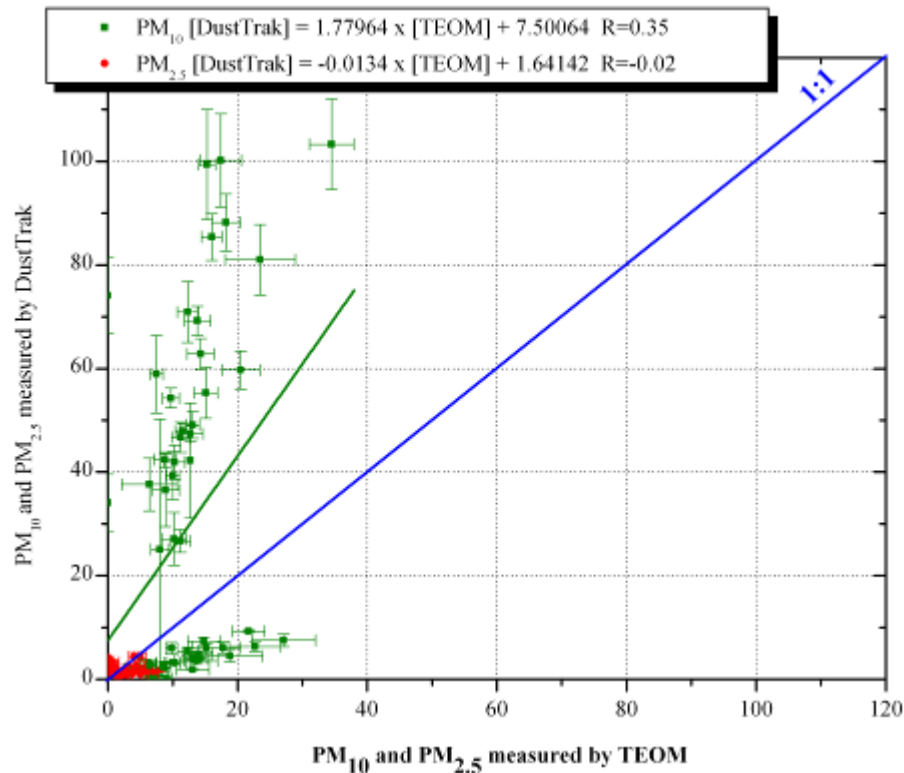


Figure 14. Comparison of 24-h PM₁₀ and PM_{2.5} mass concentrations measured by TEOM and DUSTTRAK. Error bars represent the standard error of the mean.

Comparison of Filter to Continuous Results

Figure 15 and 16 show the relationships between PM_{10} and $\text{PM}_{2.5}$ measured by TEOM/DUSTTRAK and FRM filter-based methods. The temporal correlations between PM_{10} and $\text{PM}_{2.5}$ measurements by TEOM, DUSTTRAK, and filter methods were good, with correlation coefficients from 0.62 to 0.82 (with the exception of PM_{10} DUSTTRAK). The slopes for $\text{PM}_{2.5}$ measured by TEOM and DUSTTRAK were 0.66425 and 0.29909, respectively, with insignificant intercepts. The slopes between TEOM/DUSTTRAK and filter-based PM_{10} measurements were 0.8663 for TEOM and 1.27283 for DUSTTRAK, while relatively high intercepts are computed.

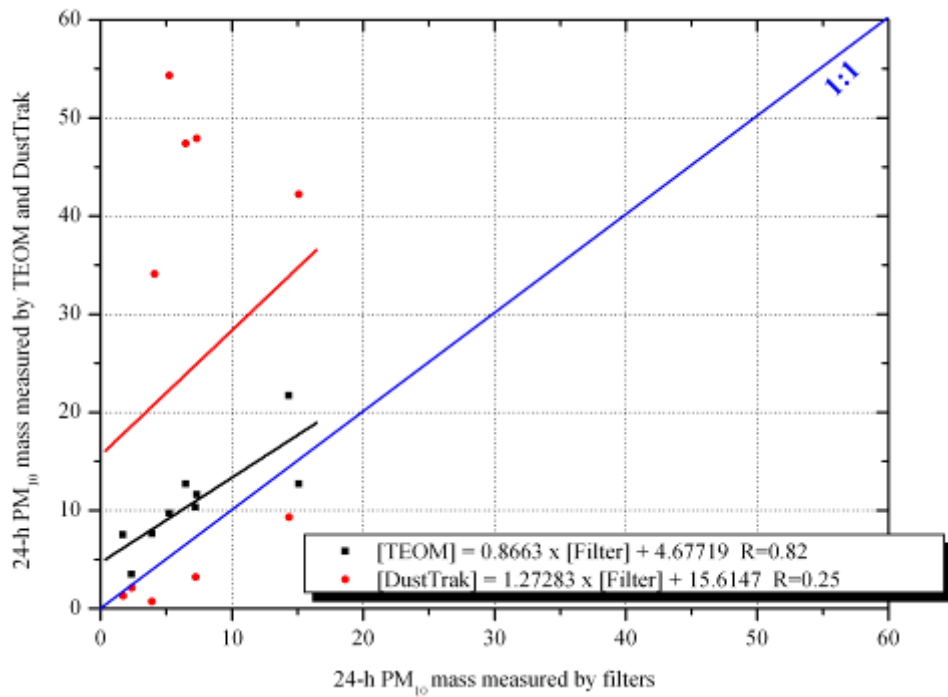


Figure 15. Relationships between PM_{10} concentrations ($\mu\text{g}/\text{m}^3$) measured by TEOM, DUSTTRAK, and filter-based methods.

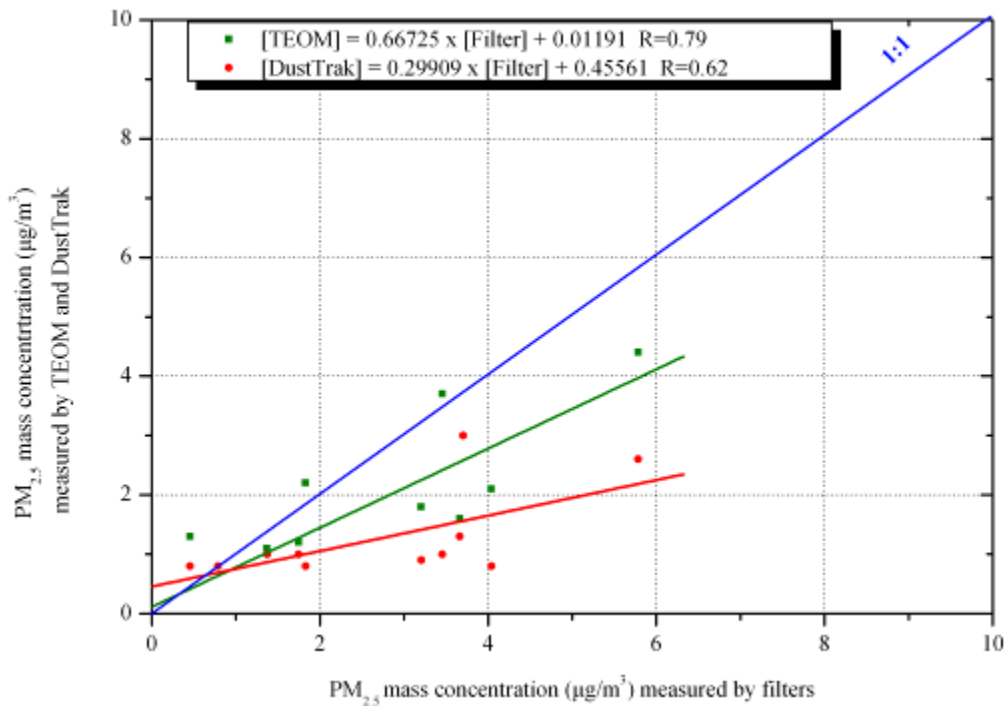


Figure 16. Relationships between PM_{2.5} concentrations ($\mu\text{g}/\text{m}^3$) measured by TEOM, DUSTTRAK, and filter-based methods.

METEOROLOGY

Variations of hourly data for each meteorological parameter are presented in Figure 17 through Figure 21. Descriptive statistics of hourly data also are presented in Table 5. Solar radiation progressively increased up to 69.9 watts/m² (Figure 17). Ambient temperature varied from 11.3 to 74.7°F with a mean temperature of 42.5°F for the monitoring period (Table 5; Figure 18). Relative humidity remained lower than 45 percent. Two rainfall events adding up 0.41 mm were recorded (Figure 19).

Table 5. Descriptive statistics of 1-hour meteorological data.

| | Mean | Minimum | Maximum | Sum |
|---|------|---------|---------|------|
| Solar radiation (watts/m ²) | 18.4 | 0.0 | 81.8 | |
| Wind speed (miles/h) | 7.5 | 0.6 | 22.9 | |
| Temperature (°F) | 54.2 | 21.4 | 85.2 | |
| Relative humidity (%) | 33.3 | 6.5 | 93.5 | |
| Precipitation (mm) | | | | 0.85 |

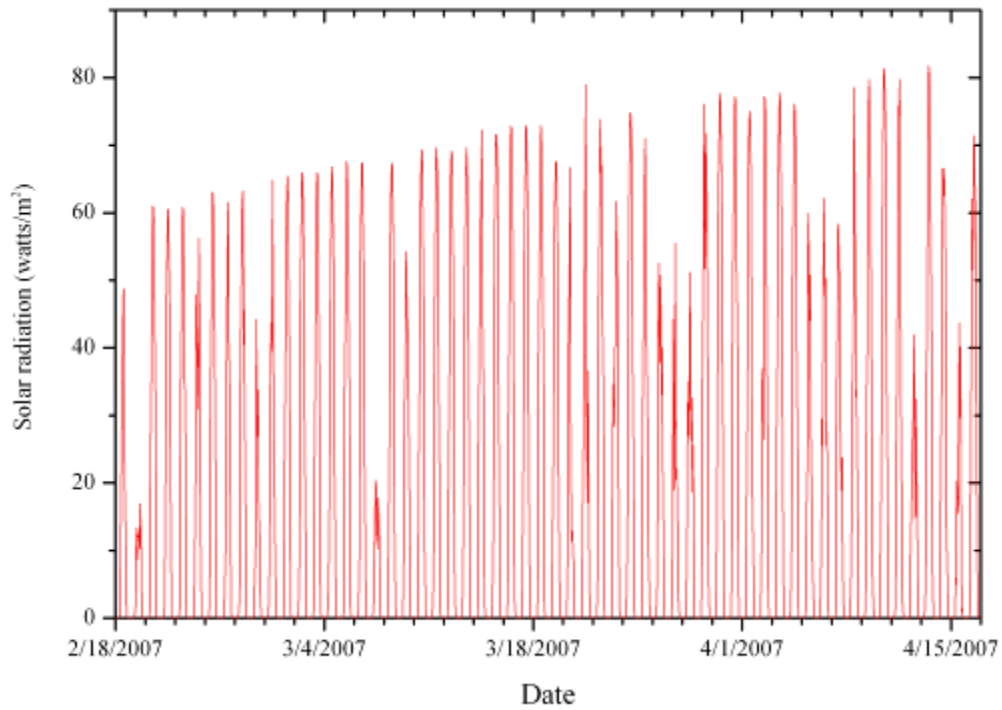


Figure 17. Solar radiation (in watts/m²) at Site #6 (Pahranagat NWR).

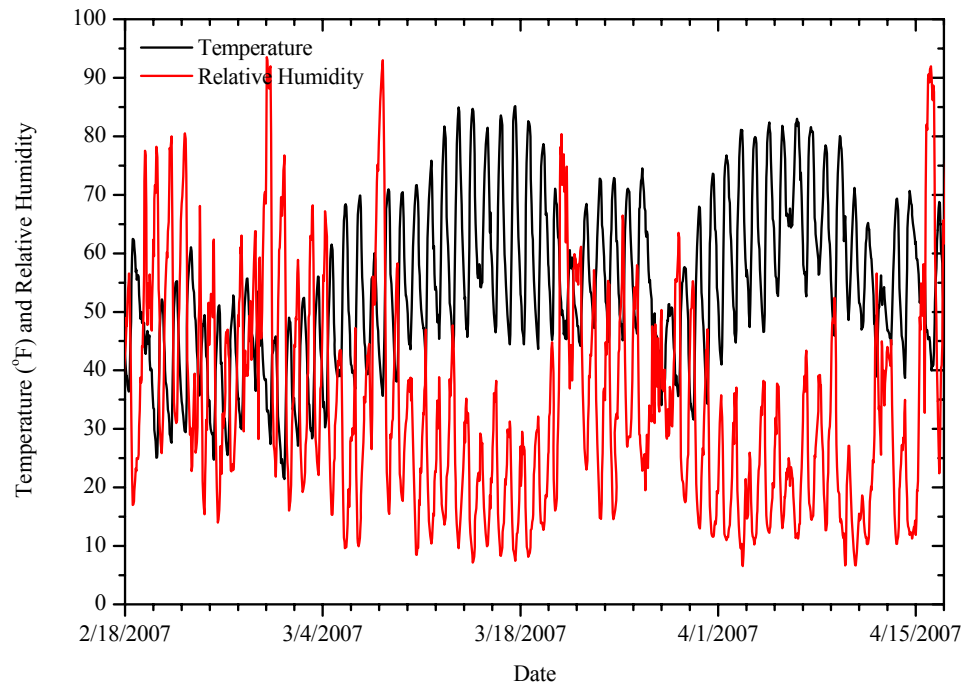


Figure 18. Temperature (in °F) and relative humidity at Site #6 (Pahranagat NWR).

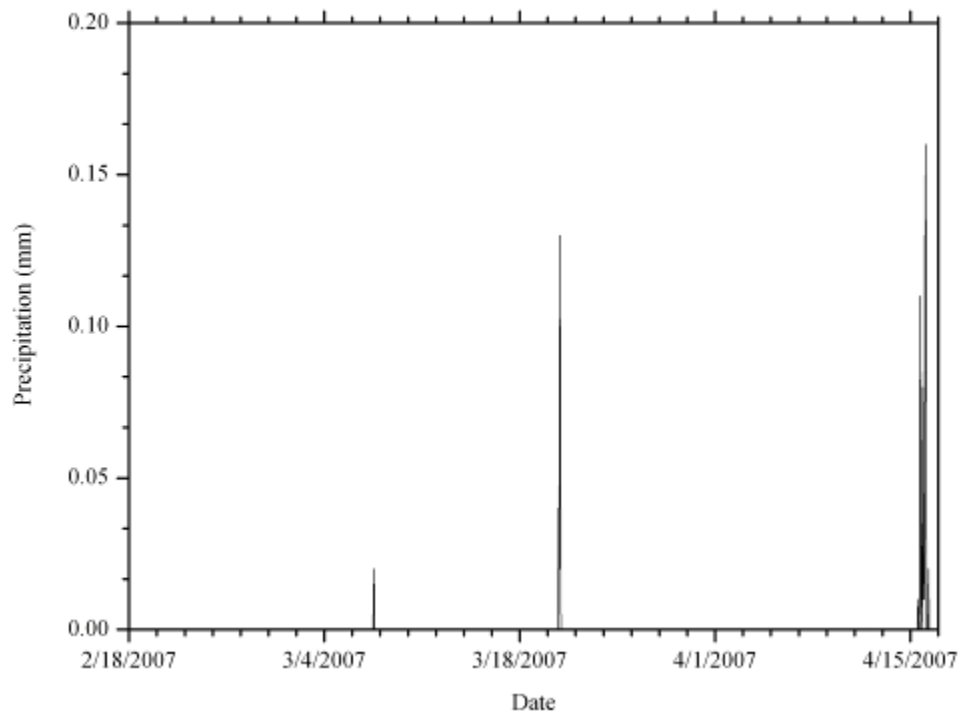


Figure 19. Total precipitation (in mm) at Site #6 (Pahranagat NWR).

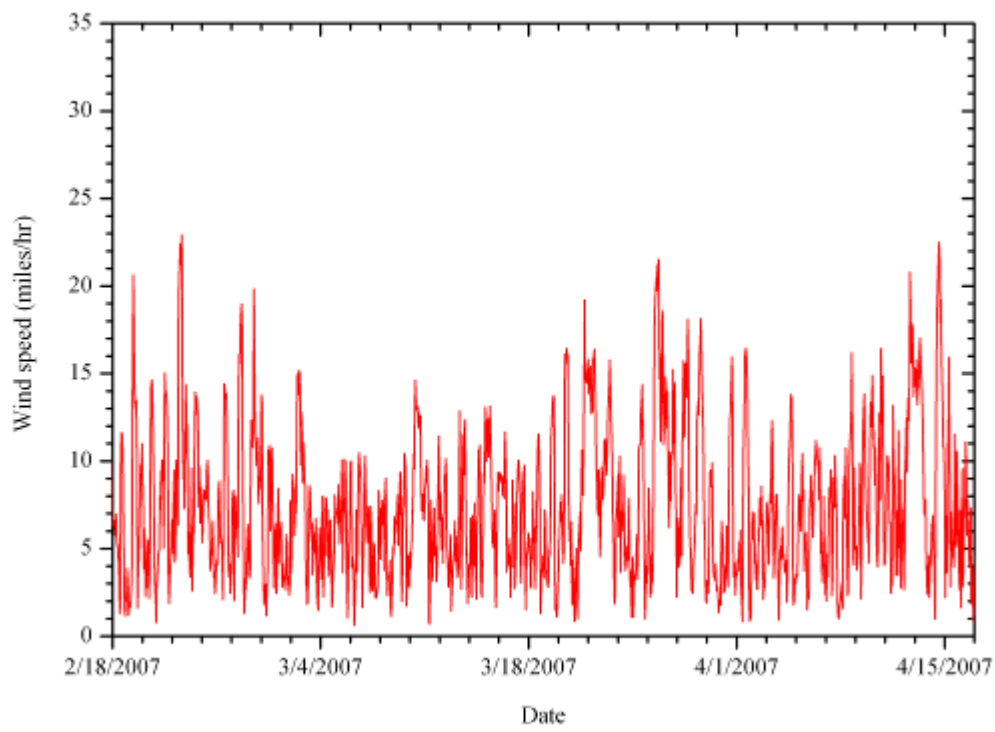


Figure 20. Wind speed (in miles/hr) at Site #6 (Pahranagat NWR).

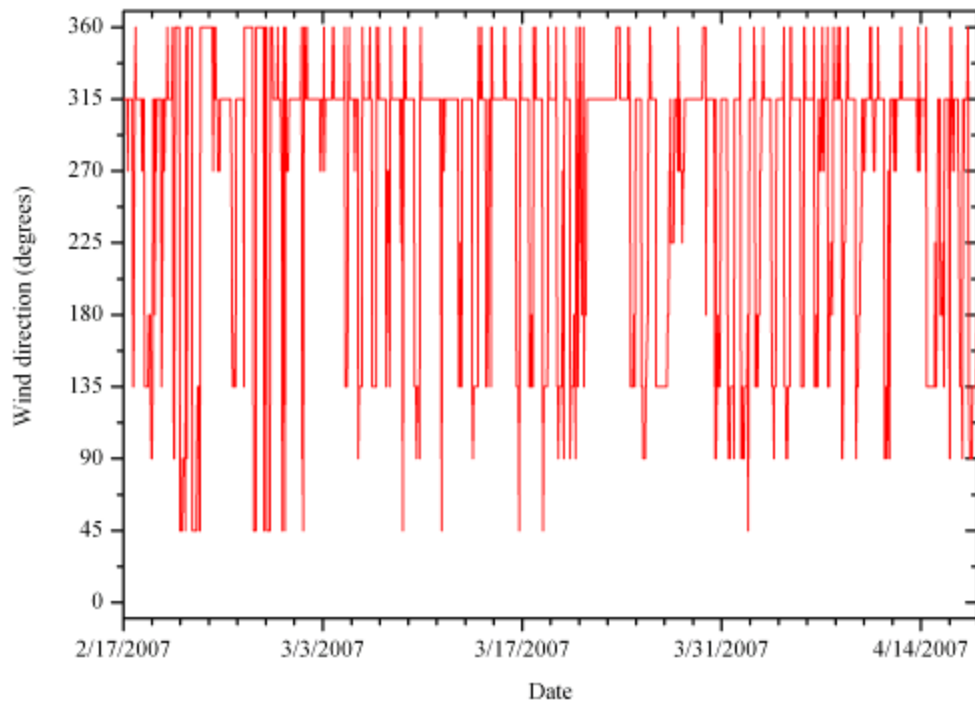


Figure 21. Wind direction at Site #6 (Pahranagat NWR).

Wind conditions for the monitoring period were described by north/northwest winds during the night and southeast winds during the day with wind speeds mostly in the range of 5 to 15 miles/hour (Figure 20 and Figure 21). The classification of wind conditions was retrieved from the Federal Meteorological Handbook (Table 6). The mean wind speed for each direction bin (8 bins) is presented in Figure 22.

Table 6. Wind condition classifications.

| Miles/hour | Specification |
|------------|---|
| <1 | Calm; smoke rises vertically. |
| 1 to 5 | Direction of wind shown by smoke drift not by wind vanes. Wind felt on face; leaves rustle; vanes moved by wind. |
| 5 to 9 | Leaves and small twigs in constant motion; wind extends light flag. |
| 9 to 14 | Raises dust, loose paper; small branches moved. |
| 14 to 23 | Small trees in leaf begin to sway; crested wavelets form on inland waters. Large branches in motion; whistling heard in overhead wires; umbrellas used with difficulty. |
| 23 to 35 | Whole trees in motion; inconvenience felt walking against wind. Breaks twigs off trees; impedes progress. |
| 35 to 48 | Slight structural damage occurs. Trees uprooted; considerable damage occurs. |
| >48 | Widespread damage. |

(retrieved from Federal Meteorological Handbook; Chapter 5. Wind;
<http://www.nws.noaa.gov/oso/oso1/oso12/fmh1/fmh1ch5.htm#chp5link>)

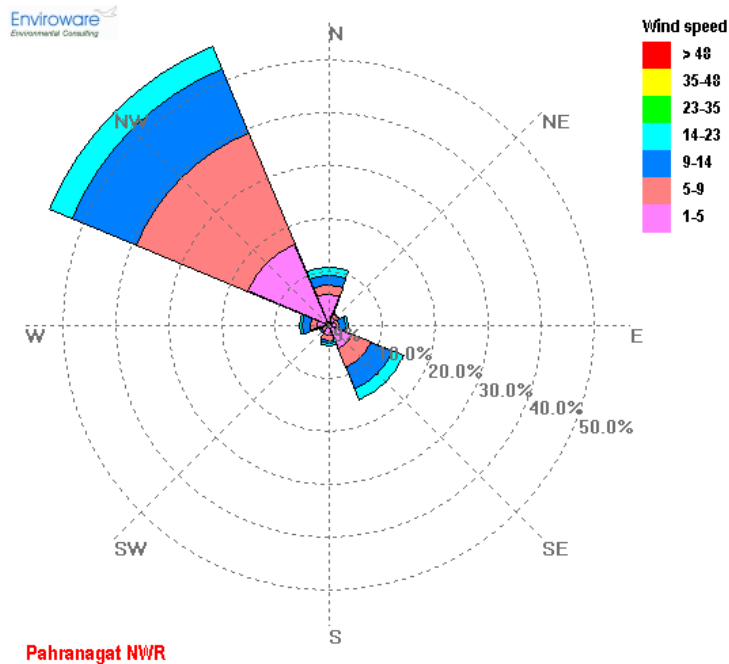


Figure 22. Wind direction and speed at Pahranagat NWR.

For the monitoring period, prevailing winds were from the northwest. Less than 3 percent of southeast winds were associated with wind speeds higher than 14 miles/hour, with a mean wind speed of 8.9 miles/hour. This is controlled by the topography of the region. Lower wind speeds are recorded for winds from the northeast (mean wind speed of 3 miles/hour) (Figure 23).

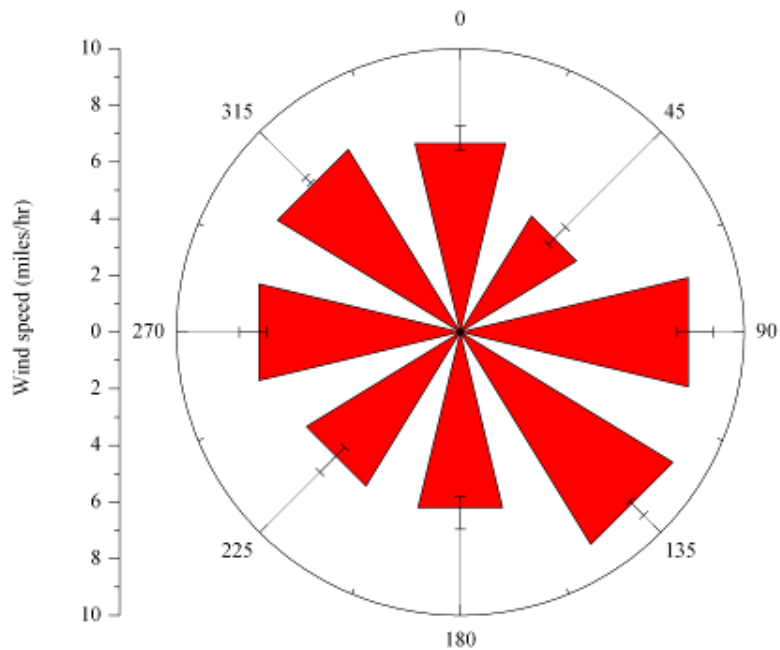


Figure 23. Average wind speed for each wind direction sector. Error bars represent the standard error of the mean.

Associations of Meteorology with Aerosol Measurements

Trends and correlations of PM mass with meteorological conditions are shown for hourly TEOM data. The increase in wind speed triggered higher PM₁₀ concentrations but a gradual decrease on PM_{2.5} concentrations. A rather bimodal pattern is observed for both fractions of particle mass (Figure 24). The first mode is associated with comparatively higher particle mass concentration in early morning (5:00 to 6:00) followed by a gradual decrease. A second, less pronounced mode can be observed in late afternoon (18:00 to 20:00), especially for the fine fraction. There are no significant differences of PM_{2.5} concentrations for different wind directions, while somewhat higher PM₁₀ levels were determined for southerly winds as compared to those blowing from the north (Figure 25 and Figure 26).

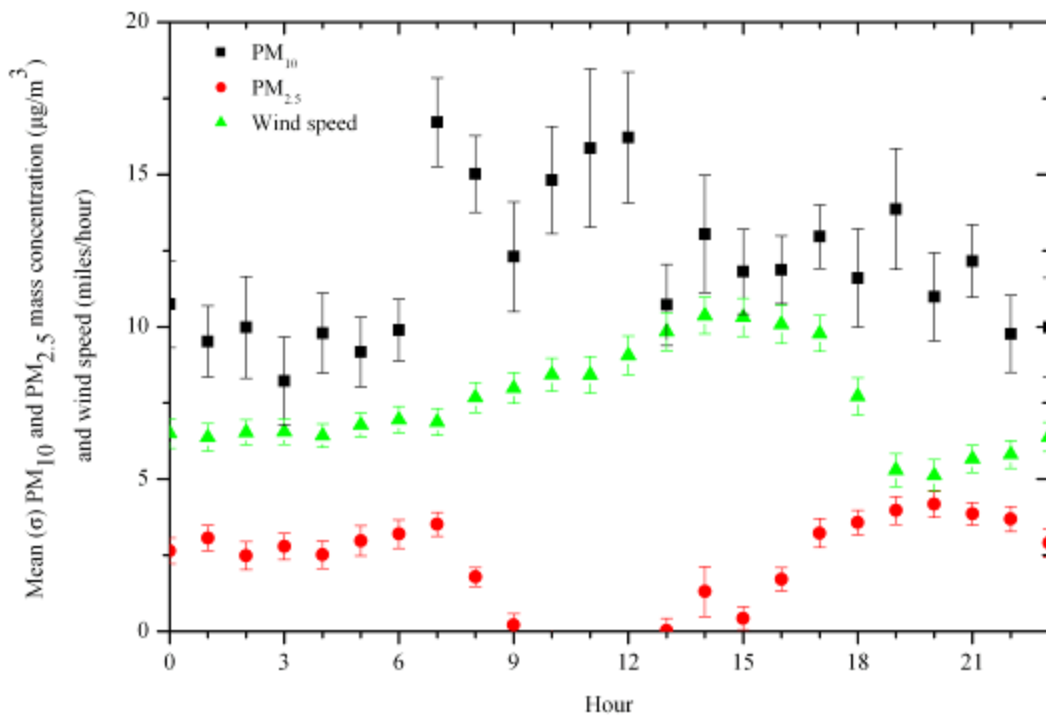


Figure 24. Hourly variation of PM₁₀ and PM_{2.5} mass concentrations ($\mu\text{g}/\text{m}^3$) as well as wind speed (miles/hour) at Site #6 (Pahranagat NWR). Error bars represent the standard error of the mean.

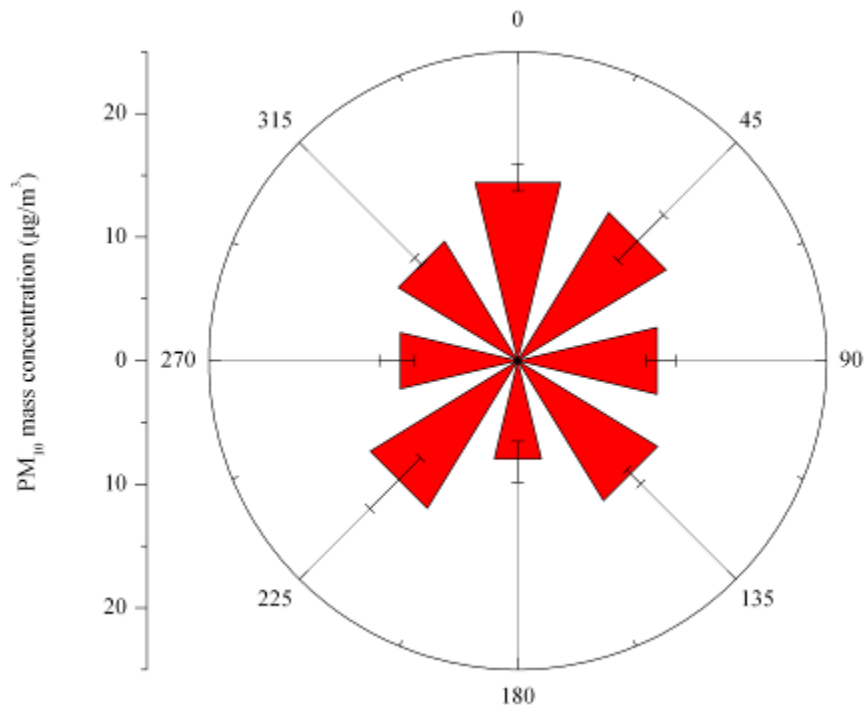


Figure 25. Mean (\pm st.error) of PM₁₀ mass concentrations ($\mu\text{g}/\text{m}^3$) for different wind direction sectors at Site #6 (Pahrangat NWR).

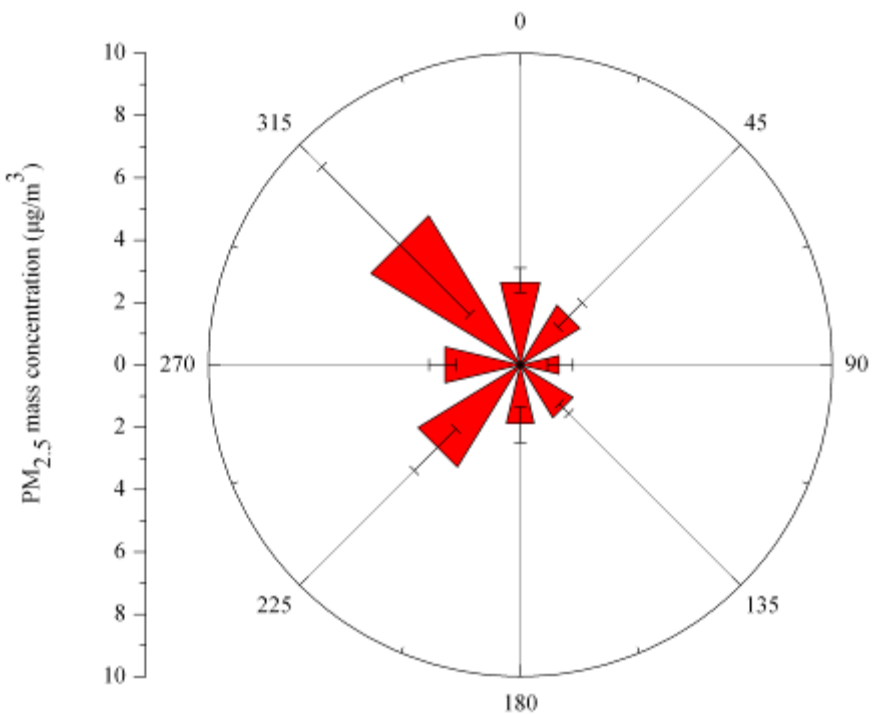


Figure 26. Mean (\pm st.error) of PM_{2.5} mass concentrations ($\mu\text{g}/\text{m}^3$) for different wind direction sectors at Site #6 (Pahrangat NWR).

CONCLUSIONS

PM₁₀ and PM_{2.5} mass concentrations and meteorological conditions were continuously monitored in the Pahranagat NWR from February 17 to April 18, 2007. At the same time, integrated samples of PM₁₀ and PM_{2.5} were collected on a 1-to-6-day schedule using FRM samplers. Two sets of filters (March 19 and April 6, 2007) were analyzed for major anions (sulfate, nitrate, chloride) and cations (sodium and potassium), elements (from sodium to uranium), and elemental and organic carbon. The comparison of PM₁₀ and PM_{2.5} mass concentrations obtained by continuous monitors and filters showed that differences are associated with the limitations of the instrumentation. For example, while light scattering (the measurement technique for DUSTTRAK) is not influenced by volatilization losses and is accurate for fine particles, it performs poor for coarse particles, resulting in underestimation of PM₁₀ mass. TEOM PM₁₀ measurements were subject to volatilization artifacts at relatively high PM₁₀ concentrations. PM_{2.5} mass measurements obtained by TEOM, DUSTTRAK, and filter-based methods were comparable.

Mean 24-h PM₁₀ and PM_{2.5} mass concentrations were 12.2 and 2.3 $\mu\text{g}/\text{m}^3$, which are significantly lower than the 24-h and annual NAAQS standards (24-h PM₁₀: 150 $\mu\text{g}/\text{m}^3$, 24-h PM_{2.5}: 35 $\mu\text{g}/\text{m}^3$; Annual PM_{2.5}: 15 $\mu\text{g}/\text{m}^3$). Higher PM₁₀ mass concentrations in the early morning indicated the possible contribution of mechanically generated coarse particles from operations on the refuge. The chemical composition of both PM₁₀ and PM_{2.5} samples indicated that organic carbon is the major component of both fractions, while soil contributes less than 50 percent of PM₁₀ mass. Sulfate and nitrate account for about 10 percent. Increases in PM₁₀ and PM_{2.5} mass concentrations are associated with higher concentrations of soil and to a lesser extent of organic mass and ammonium sulfate.

ACKNOWLEDGEMENTS

Authors thank the Pahranagat NWR for hosting the trailer on its property and for providing electricity to the trailer.

REFERENCES

Engelbrecht, J.P., I.G. Kavouras, D. Campbell, S.A. Campbell, S. Kohl, and D. Shafer, 2007a. Yucca Mountain Environmental Monitoring Systems Initiative. Air Quality Scoping Study for Ash Meadows National Wildlife Refuge, Nevada. Letter Report DOE/NV/26383-LTR2007-01

Engelbrecht, J.P., I.G. Kavouras, D. Campbell, S.A. Campbell, S. Kohl, and D. Shafer, 2007b. Yucca Mountain Environmental Monitoring Systems Initiative. Air Quality Scoping Study for Beatty, Nevada. Letter Report DOE/NV/26383-LTR2007-02

Engelbrecht, J.P., I.G. Kavouras, D. Campbell, S.A. Campbell, S. Kohl, and D. Shafer, 2007c. Yucca Mountain Environmental Monitoring Systems Initiative. Air Quality Scoping Study for Rachel, Nevada. Letter Report DOE/NV/26383-LTR2007-03

Engelbrecht, J.P., I.G. Kavouras, D. Campbell, S.A. Campbell, S. Kohl, and D. Shafer, 2007d. Yucca Mountain Environmental Monitoring Systems Initiative. Air Quality Scoping Study for Sarcobatus Flats, Nevada. Letter Report DOE/NV/26383-LTR2007-04

Kavouras, I.G., N. Mihalopoulos, and E.G. Stephanou, 1998. Formation of atmospheric particles from organic acids produced by forests. *Nature*, 395, 683-686.

Kavouras, I.G., N. Mihalopoulos, and E.G. Stephanou, 1999. Secondary organic aerosol formation vs. primary organic aerosol emissions: In situ evidence for the chemical coupling between monoterpane acidic photo-oxidation products and new particle formation over forests. *Environmental Science and Technology*, 7, 1028-1037.

Kavouras, I.G., V. Etyemezian, D. DuBois, J. Xu, M. Pitchford, and M. Green, 2005. Assessment of the Principal Causes of Dust-Resultant Haze at IMPROVE Sites in the Western United States. Final report to Western Regional Air Partnership (www.coha.dri.edu/dust).

Lefer, B.L. and R.W. Talbot, 2001. Summertime measurements of aerosol nitrate and ammonium at a northeastern U.S. site. *Journal of Geophysical Research*, 106, 20,365-20,378.

Malm, W.C., B.A. Schichtel, R.B. Ames, and K.A. Gebhart, 2002. A 10-year spatial and temporal trend of sulfate across the United States. *Journal of Geophysical Research*, 107, 4627, doi:10.1029/2002JD002107.

Malm, W.C., B.A. Schichtel, M.L. Pitchford, L.L. Ashbaugh, and R.A. Eldred, 2004. Spatial and monthly trends in speciated fine particle concentration in United States. *Journal of Geophysical Research*, 109, D03306, doi:10.1029/2006JD003739.

White, W.H. and P.T. Roderts, 1977. On the nature and origins of visibility-reducing aerosol in the Los Angeles air basin. *Atmospheric Environment*, 11, 803-812.